

# Modulus Ratio and Joint Factor Concepts to Predict Rock Mass Response

T. Ramamurthy<sup>1</sup> · G. Madhavi Latha<sup>2</sup> · T. G. Sitharam<sup>2</sup>

Received: 27 April 2015 / Accepted: 6 October 2016 / Published online: 22 October 2016  
© Springer-Verlag Wien 2016

**Abstract** The commonly adopted rock mass classifications, namely RMR,  $Q$  and GSI, are used to estimate compressive strength and modulus of rock masses. These values have been examined as per modulus ratio concept,  $M_{rj}$ , for their reliability. The design parameters adopted in some of the recent case studies based on these classifications indicate that the  $M_{rj}$  values for rock masses are higher than those of the corresponding intact rocks. The joint factor,  $J_f$ , which is defined as a weakness coefficient in rock mass suggests that modulus ratio of rock mass ( $M_{rj}$ ) has to be less than the modulus ratio of the corresponding intact rock ( $M_{ri}$ ), on the basis of extensive experimental evidence. With joint factor, compressive strength, elastic modulus, cohesion and friction angle were estimated and applied in the analyses of a few cases. The predictions of deformations with this approach agreed well with the field measurements by adapting equivalent continuum approach. The modulus ratio concept is considered to present a unified classification for intact rocks and rock masses. Soil–rock boundary, standup time in under ground excavations and also penetration rate of TBM estimates have been linked to  $M_{rj}$ .

**Keywords** Case studies · Classification · Joint factor · Modulus ratio · Numerical modeling · Penetration rate of TBM · Rock mass properties · Standup time

## 1 Introduction

Laboratory testing is not easy in the case of rock masses. Rocks are usually discontinuous, non-homogeneous, anisotropic and prestressed. Collection of undisturbed specimens of rock mass to test in laboratory is considered to be uneconomical and mostly not practicable. In some cases, large field shear and plate loading tests are conducted to assess rock mass properties. These tests are time consuming and expensive. Hence, it is a common practice to conduct tests on intact rock specimens in a laboratory to arrive at the upper bound values of rock parameters. Attempts have been made to correlate strength and modulus of intact rock with those of rock mass through rock mass classifications. These correlations have often been adopted to assess compressive strength ( $\sigma_{cj}$ ), modulus ( $E_j$ ), cohesion ( $c_j$ ) and friction angle ( $\phi_j$ ) and to predict stress–strain response of rock mass.

The rock mass classifications, RMR by Bieniawski (1973),  $Q$ -system by Barton et al. (1974) have been in practice to estimate the compressive strength and modulus of rock mass. In fact, these two important parameters of rock mass have not been assessed from actual tests in unconfined condition. With number of tests conducted on jointed rocks and rock-like materials in unconfined condition (Ramamurthy 1993; Ramamurthy and Arora 1994), a weakness coefficient, called joint factor ( $J_f$ ), was evolved to account for the combined influence of number of joints, critical joint inclination and the strength along this joint. Uniaxial compressive strength and modulus were linked to

✉ G. Madhavi Latha  
madhavi@civil.iisc.ernet.in

T. Ramamurthy  
temuraramamurthy@yahoo.com

T. G. Sitharam  
sitharam@civil.iisc.ernet.in

<sup>1</sup> Angron Geotech Pvt. Ltd, Naraina Industrial Area, Phase II, New Delhi 110025, India

<sup>2</sup> Civil Engineering Department, Indian Institute of Science, Bengaluru 560012, India

$J_f$ , which also suggested that the modulus ratio of jointed specimens decreased with the increase in  $J_f$ , i.e., with the decreasing quality of specimens, small and large. With the experimental finding, RMR, Q and GSI predications of  $M_r$  found to be much higher than those of corresponding intact rocks. A few case studies have been examined with  $J_f$  relations, and good rock mass responses were predicted. Based on  $J_f$  finding, a unified classification for intact and jointed rocks is suggested with  $M_r$  which is also incorporated in equations to estimate the standup time and penetration rate of TBMs.

## 2 Modulus Ratio Concept

Hypothetical stress–strain curves for three different rocks are presented in Fig. 1. Curves OA, OB and OC represent three stress–strain curves with failure occurring at A, B and C, respectively. Curves OA and OB have same modulus but different strengths and strains at failure, whereas the curves OA and OC have same strength but different moduli and strains at failure. So neither strength nor modulus alone could be chosen to represent the overall quality of the rock. Therefore, strength and modulus together will give a realistic understanding of the rock response for engineering usage. This approach to define the quality of intact rocks was proposed by Deere and Miller (1966) by considering the modulus ratio ( $M_{ri}$ ), which is defined as the ratio of tangent modulus of the intact rock ( $E_i$ ) at 50 % of failure strength and its compressive strength ( $\sigma_{ci}$ ).

The classification of intact rocks presented by Deere and Miller (1966) was based on laboratory tests of 613 rock specimens from different locations covering 176 igneous,

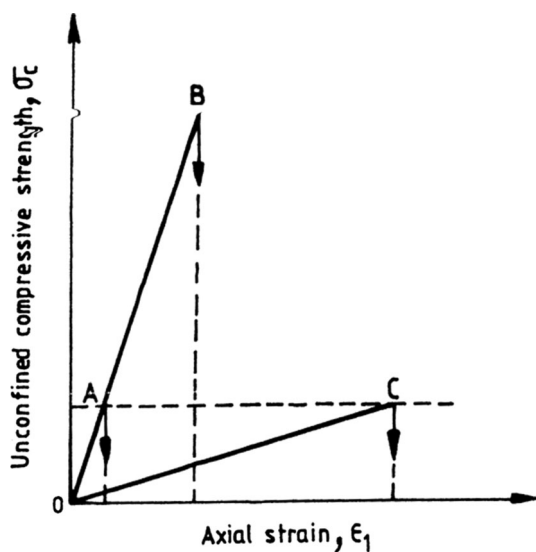


Fig. 1 Hypothetical stress–strain curves

193 sedimentary, 167 metamorphic and 77 limestones and dolomites to classify intact rocks on the basis of  $\sigma_{ci}$  and modulus ratio,  $M_{ri}$ . It was found that for basalts and limestones, one could expect  $M_{ri}$  values up to 1600, whereas for shales, this value could be close to 60. Even weathered Keuper Marl showed  $M_{ri}$  close to 50 (Hobbs 1975).

## 3 Rock Mass Parameters from Classifications

At present RMR, Q and GSI approaches are the most commonly adopted rock mass classifications. Significant contributions have come from Bieniawski (1973) and Barton et al. (1974) based on empirical approaches for the design of tunnels. GSI classification by Hoek (1994) and Hoek and Brown (1997) was a combination of RMR and Q approaches with some modification. Initially, the values of GSI were same as RMR as suggested by Bieniawski (1976) for RMR >18, and for GSI <18, Q values were considered for the rock mass. Often designers adopt one or more classifications to obtain design parameters to arrive at a conservative design.

### 3.1 Strength and Modulus from RMR

Bieniawski (1973) suggested shear strength parameters,  $c_j$  (cohesion) and  $\phi_j$  (friction angle), for five rock mass classes. These parameters have been in use for over four decades. With these values of  $c_j$  and  $\phi_j$ , the uniaxial compressive strength ( $\sigma_{cj}$ ) of a rock mass is calculated as per Mohr–Coulomb criterion given by Eq. (1) and presented in Table 1.

$$\sigma_{cj} = 2c_j \cos \phi_j / (1 - \sin \phi_j). \tag{1}$$

Table 1 also includes the estimated values of  $E_j$  as per the following equation given by Serafim and Pereira (1983)

$$E_j = 10^{(RMR-10)/40}, \text{ GPa}. \tag{2}$$

It is obvious from Table 1 that the modulus ratios decrease with the decrease of RMR, but the values are extremely high for rock masses, as compared to intact rocks (Deere and Miller 1966).

Table 1  $M_{ri}$  values with RMR for rock masses

RMR	$\sigma_{cj}$ (MPa)	$E_j$ (GPa)	$E_j/\sigma_{cj}$
100	3.5 <sup>a</sup>	177.80	50,800
80	1.97	56.20	28,528
60	1.18	17.80	15,085
40	0.64	5.60	8750
20	0.26	1.78	6846

<sup>a</sup> Value by extrapolation;  $E_j$  from Serafim and Pereira (1983)

### 3.2 Strength and Modulus from $Q$

Barton (2002) suggested modification to the earlier  $Q$  values given by Barton et al. (1974) by considering the influence of uniaxial compressive strength of the intact rock ( $\sigma_{ci}$ ) as shown in Eq. (3) and recommended  $Q_c$  values for estimating the compressive strength and modulus of rock mass as follows.

$$Q_c = Q\sigma_{ci}/100 \tag{3}$$

$$\sigma_{cj} = 5\gamma Q_c^{1/3}, \text{ MPa} \tag{4}$$

$$E_j = 10Q_c^{1/3}, \text{ GPa}, \tag{5}$$

where  $\gamma$  is the density of rock mass in g/cc. Equation (4) suggests that  $Q_c$  is linked to the compressive strength of the rock mass through the intact rock strength. On the contrary, the modulus of rock mass,  $E_j$ , is not linked to the modulus of the intact rock through  $Q_c$ .

Another important recommendation of Barton (2002) is to assess  $c_j$  and  $\phi_j$  of rock mass from the following expressions,

$$c_j = (RQD/J_n)(1/SRF)(\sigma_{ci}/100) \tag{6}$$

$$\phi_j = \tan^{-1}(J_r J_w / J_a), \tag{7}$$

where  $J_n$  is joint set number as per Barton, SRF is the stress reduction factor,  $J_r$  is joint roughness number,  $J_w$  is for seepage and its pressure and  $J_a$  is joint alteration number.

With the data provided by Barton (2002), the values of compressive strengths of rock mass are calculated as per Mohr–Coulomb criterion using  $c_j$  and  $\phi_j$  and are referred to as  $\sigma_{cj2}$  in Table 2 in this paper. These data suggest that  $\sigma_{cj2}$  values differ significantly from the suggested values of  $\sigma_{cj1}$  calculated using Eq. (4). The ratio of  $\sigma_{cj1}$  and  $\sigma_{cj2}$  varies from 1:7 to 54:1 depending upon the value of  $Q_c$ . Barton (2002) also presented the values of  $E_j$ . The values of modulus ratio,  $M_{rj}$ , are more or less constant and are around 800. In fact, Eqs. (4) and (5) give this ratio as 800

for a rock mass density of 2.5 g/cc, irrespective of  $Q_c$  varying from 0.001 to 1000, i.e., whether the rock is intact, jointed, isotropic or anisotropic.

### 3.3 Strength and Modulus from GSI

Hoek (1994) and Hoek and Brown (1997) advocate the adoption of Geological Strength Index, GSI, to estimate the material parameters,  $m_j$  and  $s_j$ , of the Hoek–Brown failure criterion to predict strength under any desired confining pressure. GSI is based on both RMR and Q-systems with some modifications mainly to estimate the compressive strength of rock mass. Their original expression for compressive strength is given as

$$\sigma_{cj}/\sigma_{ci} = \sqrt{s_j}; s_j = \exp[(GSI - 100)/9]. \tag{8}$$

There have been modifications subsequently to estimate  $s_j$  and  $\sqrt{s_j}$  by considering disturbance factor, D. For estimating the deformation modulus, Hoek (1994) recommended the use of Eq. (2) using RMR as per Bieniawski (1973) and not the GSI value. More recently, Hoek et al. (2002) suggested estimation of  $\sigma_{cj}$  and  $E_j$  in terms of disturbance factor, D, and GSI.

The values of GSI,  $s_j$  and  $E_j$  given by Hoek (1994) have been considered for calculating the values of modulus ratio,  $M_{rj}$ , in Table 3 of this paper. The values of  $M_{rj}$  are surprisingly high, ranging from 1500 to 1720 with an average value of 1621 for GSI varying from 85 to 34. These values of  $M_{rj}$  do not decrease with the decrease of GSI value. Equations given by Hoek et al. (2002) also suggest high  $M_{rj}$  values, but lower than Hoek (1994).

## 4 Parameters Used in Case Studies

The design parameters, i.e., compressive strength and modulus of rock masses adopted in some of the recent projects based on rock mass classifications, have been

**Table 2** Values of  $\sigma_{cj}$ ,  $c_j$ ,  $\phi_j$  and  $E_j$  as per Barton (2002) for  $\sigma_{ci} = 100$  MPa,  $\gamma = 2.5$  g/cc

$Q_c$	$\sigma_{cj1}$ (MPa)	$c_j$ (MPa)	$\phi_j^o$ (MPa)	$\sigma_{cj2}$ (MPa)	$\sigma_{cj1}/\sigma_{cj2}$	$E_j$ (GPa)	$M_{rj}$
100	58.0	50	63	412.7	1/7	46	843
10	26.9	10	45	48.3	1/1.8	22	818
1.2	13.3	2.5	26	8.0	1.7	10.7	805
0.04	4.3	0.26	9	0.61	7.0	3.5	814
0.008	1.2	0.01	5	0.022	54	0.9	750
<i>Before grouting</i>							
0.40	8.3	1.7	14	4.4	1.89	7.0	843
<i>After grouting</i>							
8.3	25	8.3	63	69	1/2.6	20.0	800

$\sigma_{cj1}$  from Barton, Eq. (4)

$\sigma_{cj2}$  from  $c_j$  and  $\phi_j$  values Eqs. (6) and (7)

**Table 3** Prediction of  $\sigma_{cj}$ ,  $E_j$  and  $M_{rj}$  for  $\sigma_{ci} = 100$  MPa; data from Hoek (1994)

GSI	$s_j$	$\sigma_{cj}$ (MPa)	$E_j$ (GPa)	$M_{rj} = E_j/\sigma_{cj}$
85	0.190	43.6	75	1720
75	0.062	24.9	40	1606
65	0.021	14.5	24	1655
62	0.015	12.2	20	1639
60	0.012	11.0	18	1636
50	0.004	6.3	10	1587
48	0.003	5.5	9	1636
40	0.0013	3.6 <sup>a</sup>	6	1667
38	0.001	3.2	5	1563
34	0.0004	2.0	3	1500
			Average	1621

<sup>a</sup> Estimated from Eq. (8)

checked with modulus ratio concept. Only those cases in which the parameter of intact and rock mass are available, have shown that  $M_{rj}$  values are much higher than  $M_{ri}$ , contrary to the experimental evidence. A brief description of these case studies follows.

(i) In the underground pump storage development of Rio Grande No. 1, Argentina, “massive gneiss” Pelado was encountered (Moretto et al. 1993). The RQD of the rock mass varied from 65 to 90 %. The modulus of intact rock,  $E_i$ , varied from 30 to 60 GPa and compression test gave  $\sigma_{ci}$  of 140 MPa. But the triaxial compression test gave  $\sigma_{ci}$  of 110 MPa with  $c_i = 20$  MPa and  $\phi_i = 50^\circ$ . The  $M_{ri}$  would range from 273 to 546 for this case. The field shear test on rock mass gave  $c_j$  of 0.34 MPa and  $\phi_j$  of  $30^\circ$  (peak) resulting  $\sigma_{cj}$  of 1.25 MPa as per Mohr–Coulomb theory. The modulus of deformation,  $E_d$ , from plate load test varied from 40 to 90 GPa from loading and unloading cycles, average being 60 GPa adopted in the analysis. Finite element (FE) and boundary element (BE) analyses were conducted with  $K_0$  varying from 0.5 to 2.0, considering the rock as elastic medium. Modulus ratio for the rock mass ( $M_{rj}$ ) is 4800 and  $M_{rj}/M_{ri}$  is 8.79 by considering the maximum  $M_{ri}$ . These values are very high. Modulus ratio reflects the quality of rock, and the quality of rock mass will be less than that of the intact rock. The  $M_{rj}/M_{ri}$  should have been less than 1.0 and may be 1/2, 1/3, 1/4 depending upon the quality of rock mass. It was reported that the measured deformations were twice the calculated values.

(ii) The rock encountered in the Masua mine, Italy, was dolomite limestone with RMR of 80,  $\sigma_{ci}$  of 87.8 MPa,  $E_i$  of 78 GPa,  $\sigma_t$  (tensile strength) of 5.6 MPa,  $c_i$  of 31 MPa,  $\phi_i$  of  $45^\circ$  and  $M_{ri}$  of 888 as per Barla (1993). From the field plate loading test for the predominantly isotropic rock,  $E_d$

varied from  $37.5 \pm 5.5$  GPa. The final RMR chosen was  $68 \pm 10.8$ , and from GSI,  $\sigma_{cj}$  estimated was  $15.8123 \pm 0.0046$  MPa. The value of  $E_j$  varied between 32 and 43 GPa with average being 37.5 GPa. The ratio  $M_{rj}/M_{ri}$  for maximum value of  $M_{rj}$  is 3.07 and for minimum is 2.28. By adopting discontinuity method for 3D analysis and FEM for 2D analysis, it was mentioned that the deformations on the hanging wall of the southern open slope were in the same range of the predicted values.

(iii) Hoek and Moy (1993) dealt with various aspects of power house caverns in weak rock. In one of these caverns, siltstone with  $\sigma_{ci}$  of 100 MPa, RMR of 48,  $E_d$  of 8.9 GPa and  $s_j$  of 0.003 was assessed. Compressive strength  $\sigma_{cj}$  calculated from the properties was 5.477 MPa. No  $E_j$  value is available. Modulus ratio of the jointed rock  $M_{rj}$  for this case was calculated as 1625 and appears to be rather high for RMR value of 48. Even by assuming a high value for  $M_{ri}$ , say 500,  $M_{rj}/M_{ri} = 3.25$ .

(iv) Hoek and Brown (1997) recommendations indicate

- For good-quality rock (GSI = 75),  $\sigma_{cj} = 64.8$  MPa,  $E_j = 42$  GPa,  $M_{rj} = 648$
- For average-quality rock (GSI = 50),  $\sigma_{cj} = 13.0$  MPa,  $E_j = 9.0$  GPa,  $M_{rj} = 692$
- For poor-quality rock (GSI = 30),  $\sigma_{cj} = 1.7$  MPa,  $E_j = 1.4$  GPa,  $M_{rj} = 824$
- For Braden braccia, El Teniente mine, Chile GSI = 75,  $c_j = 4.32$  MPa,  $\phi_j = 42^\circ$ ,  $\sigma_{cj} = 19.4$  MPa,  $E_j = 30$  GPa,  $M_{rj} = 1546$
- For Nathpa Jhakri HE Project, India, quartz mica schist (GSI = 65),  $c_j = 2.0$  MPa,  $\phi_j = 40^\circ$ ,  $\sigma_{cj} = 8.2$  MPa,  $E_j = 13$  GPa,  $M_{rj} = 1585$
- Athens schist—decomposed, GSI = 20,  $c_j = 0.09$ – $0.018$  MPa,  $\phi_j = 24^\circ$ ,  $\sigma_{cj} = 0.27$ – $0.53$  MPa,  $E_j = 398$ – $562$  MPa,  $M_{rj} = 1060$  (min.) and 1474 (max.)
- Yacambu Quibor tunnel, Venezuela,

For poor-quality graphitic phyllite, GSI = 24,  $c_j = 0.34$  MPa,  $\phi_j = 24^\circ$ ,  $\sigma_{cj} = 1.0$  MPa,  $E_j = 870$  MPa,  $M_{rj} = 870$ .

Note:  $M_{rj}$  values are rather high; stronger rocks have lower and weaker ones have higher values.

(v) For the Mingtan Pump Storage Project, Taiwan, underground power cavern, 22 m wide, 46 m high, 158 m long, and a transformer hall, 13 m wide, 20 m high, 172 m long, are located at a depth of 300 m below the ground level in jointed sandstone and bedded sandstone (Yu and Liu 1993).

- For jointed sandstone:  $\sigma_{ci} = 166$  MPa,  $E_i = 22.3$  GPa,  $M_{ri} = 134$ .
- For bedded sandstone:  $\sigma_{ci} = 66$  MPa,  $E_i = 12.8$  GPa,  $M_{ri} = 194$ .

These are average values for intact rock cores.

The average RMR values for jointed sandstone and for bedded sandstone were 69 and 58, respectively. They have adopted for:

1. Jointed sandstone:  $\sigma_{cj} = 45\text{--}65$  MPa,  $E_j = 29.85$  GPa, so  $M_{rj} = 543$  and  $M_{rj}/M_{ri} = 4.0$ .
2. Bedded sandstone:  $\sigma_{cj} = 11.48$  MPa,  $E_j = 15.85$  GPa, so  $M_{rj} = 1381$  and  $M_{rj}/M_{ri} = 7.1$ .

When field plate loading tests were conducted, the modulus of deformations ( $E_d$ ) was much lower than the modulus as per Serafim and Pereira (1983). For the jointed sandstone,  $E_d = 4.15$  GPa, and for bedded sandstone  $E_d = 2.9$  GPa.

By adopting 2D finite difference program Fast Lagrangian Analysis of Continua (FLAC), the progressive response of rocks was considered to be elasto-plastic as per Mohr–Coulomb theory. Iterated analysis was carried out by lowering the parameters of both intact rock and jointed rocks mass, to obtain deformations to match the measured ones. Finally, computed back analysis data were as follows.

1. Jointed sandstone:

$$\sigma_{ci} = 100 \text{ MPa}, m_j = 4.298, s_j = 0.02047$$

giving  $\sigma_{cj} = 14.3$  MPa and  $E_j = 4.5$  GPa, so  $M_{rj} = 315$ ,  $M_{rj}/M_{ri} = 2.4$ .

2. For the bedded sandstone

$$\sigma_{ci} = 100 \text{ MPa}, m_j = 1.519, s_j = 0.00211$$

giving  $\sigma_{cj} = 4.59$  MPa and  $E_j = 2.5$  GPa, so  $M_{rj} = 545$ ,  $M_{rj}/M_{ri} = 2.8$ .

In both the cases of sandstones, the  $M_{rj}$  values are higher than  $M_{ri}$  values even after conducting iterative analysis to match the measured deformations.

(vi) For the large span underground storage project, a cavern 25 m wide, 12 m high and 100 m long is located in Bukit Timah granite. Rock reinforcement was adopted as per Q-system, and numerical modeling was also carried out by Zhou et al. (2003). Measurements and numerical analysis showed high horizontal stresses favouring the stability of the cavern. The upward deformation in the crown was of the order of 1.0 mm only.  $\sigma_{ci} = 108$  MPa to 225 MPa (average 164 MPa),  $E_i = 49.3$  GPa to 111.3 GPa (average 65.6 GPa). The estimated  $\sigma_{cj} = 45$  to 65 MPa (average 55 MPa) and  $E_j = 40$  to 50 GPa (average 45 GPa). The  $M_{ri} = 400$ ,  $M_{rj} = 818$  and  $M_{rj}/M_{ri} = 2.04$ , which is more than 1.0.

(vii) For 1000 MW Masjed-e-Soloiman HEPP, Iran, Stabel and Samani (2003) carried out 2D elasto-plastic hybrid FEM and BEM analyses on the powerhouse cavern, 30 m span, 50 m high and 151 m long located in mudstone

consisting of layers of conglomerate, sandstone, siltstone and claystone. The rock core properties from laboratory tests of year 1991 were:

1. Conglomerate:  $\sigma_{ci} = 57$  MPa,  $E_i = 45$  GPa, so  $M_{ri} = 789$
2. Sandstone:  $\sigma_{ci} = 67$  MPa,  $E_i = 25$  GPa, so  $M_{ri} = 373$
3. Siltstone:  $\sigma_{ci} = 39$  MPa,  $E_i = 13$  GPa, so  $M_{ri} = 333$
4. Claystone:  $\sigma_{ci} = 23$  MPa,  $E_i = 8$  GPa, so  $M_{ri} = 348$ .

In the analyses, the following properties of rock layers were chosen:

1. Conglomerate:  $\phi_j = 43^\circ$ ,  $c_j = 2.87$  MPa,  $\sigma_{cj} = 13.2$  MPa,  $E_j = 15$  GPa, so  $M_{rj} = 1136$
2. Sandstone:  $\phi_j = 38^\circ$ ,  $c_j = 1.67$  MPa,  $\sigma_{cj} = 6.85$  MPa,  $E_j = 7.0$  GPa, so  $M_{rj} = 1022$
3. Siltstone:  $\phi_j = 30^\circ$ ,  $c_j = 0.73$  MPa,  $\sigma_{cj} = 2.53$  MPa,  $E_j = 6.0$  GPa, so  $M_{rj} = 2372$
4. Claystone:  $\phi_j = 24^\circ$ ,  $c_j = 0.50$  MPa,  $\sigma_{cj} = 1.54$  MPa,  $E_j = 6.0$  GPa, so  $M_{rj} = 3896$

The  $\sigma_{cj}$  values are calculated from  $c_j$  and  $\phi_j$  as per Mohr–Coulomb criterion. Therefore, for:

1. Conglomerate:  $M_{rj}/M_{ri} = 1.44$
2. Sandstone:  $M_{rj}/M_{ri} = 2.74$
3. Siltstone:  $M_{rj}/M_{ri} = 7.12$
4. Claystone:  $M_{rj}/M_{ri} = 11.20$

These values are greater than 1.0.

(viii) The analysis of intake tunnel, Karun III, HEPP, Iran, was carried out using 2D UDEC and 3D elastic programs by Tabanrad (2003). Measured deformations agreed with the estimated values from back analysis. Back analysis was carried out using direct method UDEC software, and  $\sigma_{cj}$  and  $E_j$  were estimated. For Marly limestone/marl:  $c_j = 0.6$  MPa,  $\phi_j = 30^\circ$ ,  $\sigma_{cj} = 2.08$  MPa,  $E_j = 6.0$  GPa

By considering the average values of the rocks,  $\sigma_{ci} = 70$  MPa,  $E_i = 10.25$  GPa,  $M_{ri} = 146$  and  $M_{rj} = 2855$ , so,  $M_{rj}/M_{ri} = 19.8$ .

(ix) For the underground pumped powerhouse caverns, namely, Samragjin, Muju, Sanchung, Yangyang and Chungsong, constructed during 1973 to 2003, Lim and Kim (2003) carried out numerical analyses using computer programs based on (1) viscoelastic FEM, (2) hybrid combining FEM and BEM and (3) elasto-plastic FEM. The rock mass parameters were assumed by applying reduction factors to modulus, cohesion and friction angle as 0.16–0.55, 0.12–0.22 and 0.6–0.87, respectively, to the corresponding values of intact rock cores. Mainly Mohr–Coulomb failure criterion was adopted. Detailed calculations with the parameters adopted for the analysis gave  $M_{rj}/M_{ri}$  values for the rock masses as given in Table 4.

**Table 4** Rock types and  $M_{rj}/M_{ri}$  (*Lim and Kim 2003*)

Rock type	Cavern	$M_{rj}/M_{ri}$	Convergence (mm)
1. Granetic Gneiss	Muju	1.60	19.0
2. Porphyroblastic Gneiss	Sanchung	2.87	54.4
3. Porphyroblastic Gneiss, Granite Gneiss	Yangyang	3.83	55.0
4. Sandstone, Arkosic Sandstone	Chungsong	3.30	50.0

\* For Samragjin cavern, reduction factors were not included in their paper

(x) A stochastic analysis was carried out to estimate  $\sigma_{cj}$  and  $E_j$  of three grades of Ankara andesites by calculating the influence of correlations between relevant distributions on the simulated RMR values by Sari et al. (2010). The model was also used in Monte Carlo simulation to estimate possible ranges of the Hoek–Brown strength parameters.

From minimum strength and modulus

Grade A:  $M_{ri} = 520$ ,  $M_{rj} = 7000$ ;  $M_{rj}/M_{ri} = 13.46$

Grade B:  $M_{ri} = 470$ ,  $M_{rj} = 2113$ ;  $M_{rj}/M_{ri} = 4.50$

Grade C:  $M_{ri} = 359$ ,  $M_{rj} = 1311$ ;  $M_{rj}/M_{ri} = 3.65$ .

From maximum strength and modulus

Grade A:  $M_{ri} = 425$ ,  $M_{rj} = 1568$ ;  $M_{rj}/M_{ri} = 3.69$

Grade B:  $M_{ri} = 431$ ,  $M_{rj} = 1378$ ;  $M_{rj}/M_{ri} = 3.20$

Grade C:  $M_{ri} = 326$ ,  $M_{rj} = 963$ ;  $M_{rj}/M_{ri} = 2.95$ .

(xi) For the power house Cavern, Rogun project, Kajikistan, the deformations of roof and side walls were predicted by Bronshteyn et al. (2007) using 3D FEM with Mohr–Coulomb criterion by adopting reduced  $c_i$ ,  $\phi_i$  and  $E_i$  as indicated here

For sandstone:  $c = 3.0$  to  $1.1$  MPa ( $F.S. = 2.7$ ),  
 $\phi^\circ = 50$  to  $38$  ( $F.S.$  to  $\tan \phi : 1.53$ )  
 $E = 9000$  to  $5000$  MPa ( $F.S. = 1.4$ )  
 $M_{ri} = 546$ ,  $M_{rj} = 1109$ ;  $M_{rj}/M_{ri} = 2.03$ .

For aleurolites:  $c = 2$  to  $0.5$  MPa ( $F.S. = 4.0$ )  
 $\phi^\circ = 45$  to  $32.5$  ( $F.S.$  to  $\tan \phi : 1.56$ )  
 $E = 5500$  to  $2670$  ( $F.S. = 2.06$ )  
 $M_r = 569$ ,  $M_{rj} = 1467$ ;  $M_{rj}/M_{ri} = 2.58$ .

(xii) A 3D FEM analysis was carried out for the Waitaki dam block No. 10, New Zealand by Richards and Read (2007). The tiltmeter deformations under the block No. 10 were matched to obtain in situ modulus  $E_j$ . The ratio  $E_j/E_i$  was 0.15 for class II graywacke having GSI value of 20. This value has been found to be very high, about 5 times, even for disturbance factor,  $D = 0$  as per Hoek and Diederichs (2006). The intact rock properties were  $\sigma_{ci} = 50$  to  $60$  MPa,  $E_i = 70$  GPa;  $M_{ri} = 1167$  by considering  $\sigma_{ci} = 60$  MPa.

As per Hoek and Brown (1997) for GSI = 20,  $\sigma_{ci} = 0.704$  MPa by considering  $\sigma_{ci} = 60$  MPa,  $E_j = 10$  GPa as assessed by Richards and Read (2007),  $M_{rj} = 14,205$ , therefore,  $M_{rj}/M_{ri} = 12.2$ . As per Hoek and Diederichs (2006),  $\sigma_{cj} = 3$  MPa; therefore, for  $E_j = 10$  - MPa,  $M_{rj} = 3333$  and  $M_{rj}/M_{ri} = 2.86$ .

(xiii) To provide appropriate support in the chromite mine, Ermekov et al. (1985) carried out physical model studies by adopting equivalent material modeling with a scale of 1:50. For the horizontal working of chromite in the western Kazakhstan, three support systems were adopted, namely (1) framed arch, (2) anchor supports with framed arch and (3) injected anchored support with framed arch. The stress state at the depth of 135 m in the mine was estimated as  $\sigma_1 = 6$  MPa,  $\sigma_2 = 14$  MPa and  $\sigma_3 = 11$  MPa.

For chromite cores,  $E_i = 620$  GPa,  $\sigma_{ci} = 31$  MPa,  $M_{ri} = 2000$ . For the rock surrounding the chromite,  $\sigma_{ci} = 66$  MPa,  $E_i = 46$  GPa,  $M_{ri} = 697$ . The  $\sigma_{cj}$  of chromite =  $10$  MPa,  $E_j = 2.0$  GPa,  $M_{rj} = 200$ . For rock mass,  $\sigma_{cj} = 20$  MPa,  $E_j = 1.5$  GPa,  $M_{rj} = 75$ . Therefore, for chromite,  $M_{rj}/M_{ri} = 0.1$ , and for the rock mass,  $M_{rj}/M_{ri} = 0.11$ . The properties chosen for chromite and rock mass were not based on RMR, Q or GIS, but seem to be in order, i.e.,  $M_{rj}/M_{ri}$  values are less than 1.0.

(xiv) Read (2008), from synthetic rock mass (SRM) model study for carbonatite 2D joints, with  $\sigma_{ci} = 140$  MPa,  $E_i = 60$  GPa, resulting  $M_{ri} = 430$ , gave

1. For 20 m length of joint,  $\sigma_{cj} = 80$  MPa,  $E_j = 30$  GPa,  $M_{rj} = 375$ .
2. For 40 m length of joint,  $\sigma_{cj} = 60$  MPa,  $E_j = 25$  GPa,  $M_{rj} = 416$ .
3. For 80 m length of joint,  $\sigma_{cj} = 70$  MPa,  $E_j = 30$  GPa,  $M_{rj} = 429$ .

Here the  $M_{rj}$  values from 2D joint-simulated rocks gave slightly lower values compared to the intact material. The SRM model seems to predict compressive strength and modulus values of simulated rock mass reasonably well in 2D case indicating negligible scale effect for the lengths of joints considered.

(xv) A synthetic rock mass (SRM) approach, which can take care of anisotropy and scale effects, was adopted by

**Table 5** Results of  $\sigma_{cj}/\sigma_{ci}$  from Carvalho et al. (2002) and Ramamurthy (2001)

RMR	$\sigma_{cj}/\sigma_{ci}$ (SRM)	$J_f^*$	$\sigma_{cj}/\sigma_{ci}$
0	0.0	500	0.018
5	0.06	475	0.022
15	0.06	425	0.033
25	0.07	375	0.050
57	0.15	215	0.180
72	0.23	140	0.330
80	0.39	100	0.450
92	0.66	40	0.720
100	1.00	00	1.000

$J_f^*$  and RMR relation from  $RMR = 100 - (J_f/5)$  as per Ramamurthy (2004)

Carvalho et al. (2002) to predict unconfined compressive and triaxial strengths. Clark (2006), quoted by Lorig (2007), constructed SRM model in numerical program FLAC based on actual scaled distribution of joints, predicted strength in unconfined state with RMR covering anisotropy and scale effects as shown in Table 5. The corresponding joint factor,  $J_f$ , and strength ratios ( $\sigma_{cj}/\sigma_{ci}$ ) are also indicated. The SRM values agree reasonably well with the experimental findings based on joint factor,  $J_f$ .

From a few case studies presented in the foregoing, it is obvious that strength and modulus adopted from rock mass classifications conclusively indicate  $M_{rj}/M_{ri}$  greater than 1.0. If  $M_r$  reflects the quality of rock, the quality of rock mass is definitely lower than the quality of intact rock. One may expect  $M_{rj}/M_{ri}$  less than 1.0. The reason for high ratio could be that the  $\sigma_{cj}$  and  $E_j$  from field have not been obtained in unconfined condition (i.e., in uniaxial). This could only be verified by conducting such test in laboratory or in field.

### 5 Strength and Modulus from Joint Factor, $J_f$

Based on the extensive experimental results in uniaxial compression on jointed rocks and rock-like materials, Ramamurthy (2001) suggested the compressive strength of jointed mass close to the minimum values by Eq. (9) and the corresponding modulus by Eq. (10).

$$\sigma_{cj}/\sigma_{ci} = \exp[-0.008 J_f] \quad \text{and} \quad (9)$$

$$E_j/E_i = \exp[-0.0115 J_f], \quad (10)$$

wherein  $J_f$  is a joint factor defined by Eq. (11)

$$J_f = J_n/n.r, \quad (11)$$

where  $J_n$  = joint frequency, i.e., number of joints/meter, which takes care of RQD and joint sets and joint spacing;

$n$  = inclination parameter, which depends on the inclination of sliding plane with respect to the major principal stress direction;  $r$  = a parameter for joint strength; it takes care of the influence of closed or infilled joint, thickness of gouge, roughness, extent of weathering of joint walls and cementation along the joint. A joint or a joint set whose inclination parameter is closer to  $(45 - \phi_j/2)^\circ$  with the direction of major principal stress will be the most critical one to experience sliding at first and governs the response of jointed rock. Joint strength parameter could be assessed in terms of an equivalent value of friction angle along the critical joint as  $\tan \phi_j = \tau_j/\sigma_{nj}$  obtained from shear tests, in which  $\tau_j$  = shear strength along the joint under an expected effective normal stress,  $\sigma_{nj}$ . The values of  $n$  and  $r$  are given in Tables 6, 7 and 8. The values of  $n$  were obtained by a method of analysis of data as explained by Ramamurthy and Arora (1994), and these values are given to two decimal places as per the analysis. The values in Table 8 are suggested based on our tests on different grades of plaster of Paris, sandstones, granite, dolomites, phyllites, schists and review of others test data. The U-shaped anisotropy is

**Table 6** Values of  $n$  for different joint inclination,  $\beta^\circ$  (Ramamurthy 2001)

$\beta$ ( $^\circ$ )	Type of anisotropy	
	U-shaped	Shoulder-shaped
0	0.82	0.85
10	0.46	0.60
20	0.11	0.20
30	0.05	0.06
40	0.09	0.12
50	0.30	0.45
60	0.46	0.80
70	0.64	0.90
80	0.82	0.95
90	0.95	0.98

**Table 7** Suggested joint strength parameter,  $r$ , for filled-up joints at residual stage (Ramamurthy 2001)

Gouge material	Friction angle $\phi_j$ ( $^\circ$ )	Joint strength, $r = \tan \phi_j$
Gravelly sand	45	1.00
Coarse sand	40	0.84
Fine sand	35	0.70
Silty sand	32	0.62
Clayey sand	30	0.58
Clayey silt		
Clay—25 %	25	0.47
Clay—50 %	15	0.27

**Table 8** Suggested values of  $r$  for values of  $\sigma_{ci}$  (Ramamurthy 2001)

Compressive strength, $\sigma_{ci}$ (MPa)	Joint strength parameter, $r$	Remarks
2.5	0.30	Fine grained
5.0	0.45	
15.0	0.60	
25.0	0.70	To
45.0	0.80	
65.0	0.90	
100.0	1.00	Coarse grained

due to one parallel set of cleavages or weakness planes, such as in slates. The shoulder-shaped type is due to depositional and strongly bedded layers, as in shales and sandstones. When friction values are not available from shear tests, the same may be obtain from Table 8 based on intact rock strength. The variation of  $E_j/E_i$  with joint factor,  $J_f$ , is similar to the theoretical prediction by Walsh and Brace (1966) and Hobbs (1975) for one dimensional compression between  $E_j/E_i$  versus joint frequency,  $J_n$ . But in Eq. (10),  $J_f$  involves not only  $J_n$  but also inclination of the critical joint and the strength likely to be mobilized along this joint.

Further, the modulus ratio of the jointed mass with respect to that of the intact rock is given by the following equation.

$$M_{rj}/M_{ri} = \exp[-0.0035J_f] \tag{12}$$

Table 9 gives the estimated values of  $\sigma_{cj}$  and  $M_{rj}$  for different values of  $J_f$  varying from 0 to 500 for

**Table 9** Estimation of  $\sigma_{cj}$  and  $M_{rj}$  from  $J_f$  for  $\sigma_{ci} = 100$  MPa; assumed  $M_{ri} = 500$  for intact rock

$J_f$	$\sigma_{cj}$ (MPa)	$M_{rj}$
0	100.00	500
100	44.90	352
200	20.20	248
300	9.10	175
400	4.10	123
500	1.80	87

**Table 10** Classification of intact and jointed rocks

Class	Description	$\sigma_{cij}$ (MPa)	Description	Modulus ratio of rock $M_{ri, j}$
A	Very high strength	>250	Very high modulus ratio	>500
B	High strength	100–250	High modulus ratio	200–500
C	Moderate strength	50–100	Medium modulus ratio	100–200
D	Medium strength	25–50	Low modulus ratio	50–100
E	Low strength	5–25	Very low modulus ratio	<50
F	Very low strength	<5		

$\sigma_{ci} = 100$  MPa and  $M_{ri} = 500$  of intact rock as an example. The  $M_{rj}$  values rapidly decrease with the increase in  $J_f$ . This table suggests that the relationship between  $E_j$  and  $\sigma_{cj}$  (i.e.,  $M_{rj}$ ) can neither be taken as constant nor greater than  $M_{ri}$  when the rock mass experiences fracturing and undergoing change to a lower quality. Therefore,  $M_{rj}/M_{ri}$  will be less than 1.0 for fractured rock mass compared to that of the intact rock.

### 6 Classification Based on Strength and Modulus Ratio

Even though the original classification of Deere and Miller (1966) was suggested only for intact rocks by considering  $\sigma_{ci}$  and  $E_i$ , it was modified to classify rock masses as well by Ramamurthy (2004), as shown in Table 10. It is a two-lettered classification; first letter suggests the range of compressive strength and the second letter the range of modulus ratio. The main advantage of such a unified classification is that it not only takes into account these two important engineering properties of the rock mass, but also gives an assessment of the minimum failure strain ( $\epsilon_f$ ) which the rock mass is likely to exhibit in the uniaxial compression, where in the stress–strain response is nearly linear, as follows.

$$\text{Modulus Ratio, } M_{rj} = E_{ij}/\sigma_{cj} = 1/\epsilon_{ff} \tag{13}$$

Further, the ratio of the failure strain of the intact rock to that of the jointed rock is given by,

$$\epsilon_{fi}/\epsilon_{ff} = M_{rj}/M_{ri} = \exp(-3.50 \times 10^{-3}J_f) \tag{14}$$

On the basis of experimental data of Ramamurthy (2001), the following simpler expression was also suggested,

$$\epsilon_{ff} = 50(M_{rj})^{-0.75} \% \tag{15}$$

Figure 2 is an extended version of Deere and Miller (1966) approach and will cover very low strength to very high strength rocks. A modulus ratio of 500 would mean a minimum failure strain of 0.2 %, whereas a ratio of 50 corresponds to a minimum failure strain of 2 % as per Eq. (13). Very soft rocks and dense/compacted soils would



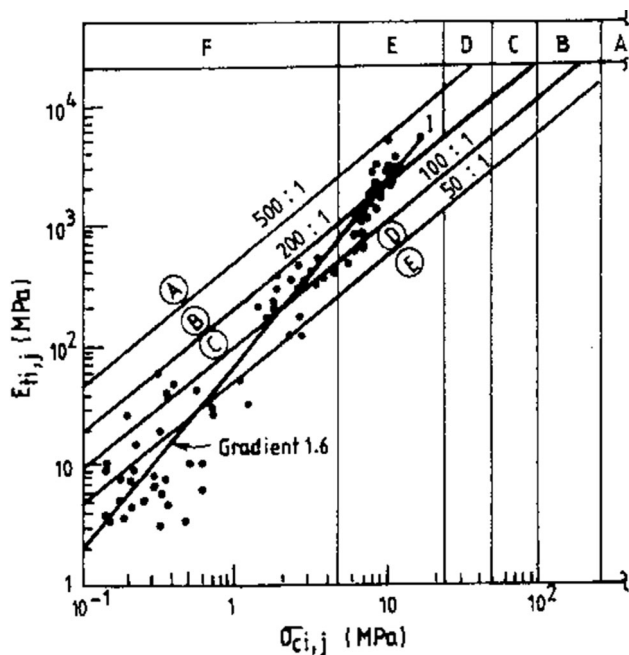


Fig. 2 Influence of jointing on modulus ratio

show often failure strains of the order of 2 %. Therefore, the modulus ratio of 50 was chosen as the lower limiting value for rocks (Ramamurthy 2004).

In Fig. 2, the location of the intact specimen is shown at ‘I’ on the  $\sigma_{ci,j}$  and  $E_{i,j}$  plot. When the experimental data of  $\sigma_{cj}$  and  $E_j$  of the jointed specimens of the same material as that of the intact specimen are plotted, all the points fall along an inclined line originating, say at ‘I’, cutting across the constant boundaries of modulus ratio. This suggests that as fracturing continues, the locations represented by  $\sigma_{cj}$  and  $E_j$  values follow a definite trend (Singh et al. 2002). These data are from a number of test specimens ( $15 \times 15 \times 15 \text{ cm}^3$ ) each of which had on an average more than 260 elemental cubes and wedge shaped elements. These specimens have undergone either sliding, shearing, splitting or rotational mode of failure.

Unconfined compression tests were also carried out on three weathered rocks, namely quartzite, granite and basalt by Gupta and Rao (2000). These three rocks have gone through different stages of weathering namely, unweathered (i.e., fresh), slightly, moderately, highly and completely weathered. These tests were carried out on quartzite that has undergone five levels of weathering and granite and basalt both undergone four levels of weathering. The values of compressive strength and modulus are presented together for these rocks in Fig. 3. The data presented suggests that the  $M_{rj}$  of jointed rock mass will be less than that of the intact rock. It is interesting to observe that the average line cuts the  $M_{rj} = 50$  line at about  $\sigma_{cj} = 1 \text{ MPa}$ . Therefore, soil–rock boundary is not only when

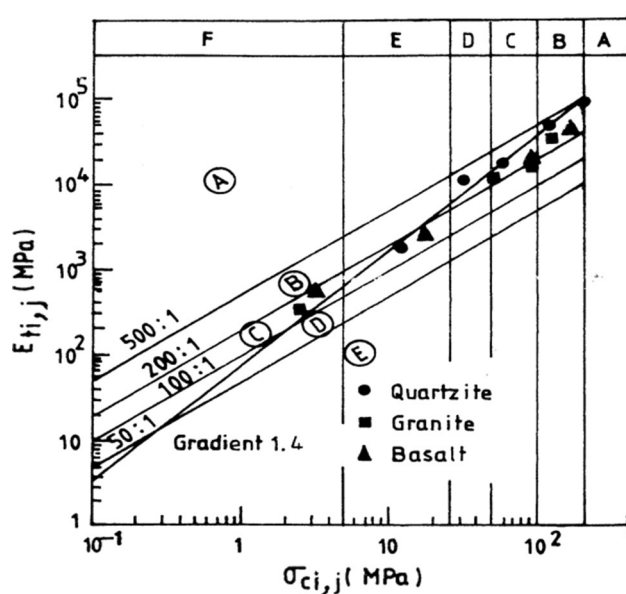


Fig. 3 Influence of weathering on modulus ratio of rocks

$\sigma_{cj} = 1 \text{ MPa}$  but also when  $M_{rj} = 50$  and  $J_f = 300$  per meter (Ramamurthy 2004).

Hence for rocks,  $\sigma_{cj}$  is greater than 1 MPa;  $M_{rj}$  is greater than 50;  $J_f$  is less than 300 per meter.

When any of these criteria do not meet the requirement of the rock mass, the mass will have to be treated as soil. Ideally when field tests are conducted, the test block is to be isolated from the parent mass by careful cutting and dressing operations to assess  $\sigma_{cj}$  and  $E_j$  in the unconstrained condition. Such a test block should have a slender ratio more than one, preferably two. Unfortunately, the data from such tests are rarely available. Whenever some data are available, it is projected to indicate the effect of the specimen size rather than the change in the quality of the rock within the test specimen/block. As the size increases, the number of joints, their inclination, even if the strength along some of the joints remains same, would affect the response of the block. If one compares a value reflected by the large-sized test blocks to that of the intact specimen, the values particularly  $\sigma_{cj}/\sigma_{ci}$  and  $E_j/E_i$  would correspond to larger values of  $J_f$ . An example is from, Natau et al. (1995) whose test results from three sizes of specimens ranging from 80 to 620 mm were obtained totally in the unconfined state. The average  $\sigma_{cj}$  and  $E_j$  obtained from these tests are presented in Table 11. From these results,  $\sigma_{cj}$  of  $620 \times 620 \times 1200 \text{ mm}^3$  specimen is 0.235 times the value of 80 mm dia. specimen. By extrapolation, for the value of compressive strength of NX size, assuming it to represent an intact rock, this ratio works out to be 0.20. The values of  $\sigma_{ci}$  of the NX size work out to be 50 MPa and  $E_i$  becomes 50 GPa. Similarly, the ratio of  $E_j$  of 620 mm specimen to the NX size is 1/20. This ratio suggests an average  $J_f$  of

**Table 11** Size effect on modulus ratio Nataou et al. (1995)

Dia. or side (cm)	$\sigma_{ci,j}$ (MPa)	$E_{i,j}$ (MPa)	$M_{ri,j}$
NX size	50.0 <sup>a</sup>	50000 <sup>a</sup>	1000
8.0	42.6	40,000	939
23.5	22.23	7500	337
62.0	10.0	2500	250

<sup>a</sup> Extrapolated from data of larger sizes

230/m from strength and modulus considerations as per Eqs. (9) and (10). The ratio  $M_{ri}$  of NX size is 1000 and the  $M_{rj}$  of 620-mm-size specimen works out to be 250, suggesting considerable change in the quality of the rock in the larger size. These data also do confirm that the  $M_{rj}$  values should decrease considerably with the decrease in the quality of the rock and not increase, remain constant or vary marginally. Earlier investigations of Rocha (1964) also suggested very low values of  $E_j/E_i$  as 1/29 for granite, 1/28 for schist, 1/64 for limestone and 1/108 for quartzite.

## 7 Influence of Confining Pressure

The field data of modulus are obtained by conducting tests on limited area in tunnels, in audits/drifts or in boreholes. Even if plate loading tests are conducted on a level surface in underground or in open excavation, there is always some degree of lateral confinement. The measured modulus values tend to be higher particularly for weaker rock masses. Such results need to be corrected for lateral confinement to obtain values corresponding to the unconfined condition. When such data are provided, the designer has the freedom to choose or modify the strength and modulus depending upon the in situ stress expected in the field. Using the following equation given by Ramamurthy (1993), the influence of confining pressure on  $E_j$  can be estimated,

$$E_{j0}/E_{j3} = 1 - \exp[-0.10\sigma_{cj}/\sigma'_3], \quad (16)$$

where the subscripts 0 and 3 refer to  $\sigma'_3 = 0$  and  $\sigma'_3 > 0$ ;  $\sigma'_3$  is the effective confining stress. For  $\sigma_{cj}$  of 5 MPa,  $\sigma'_3$  of 2 MPa,  $E_{j3}$  will be 4 times of  $E_{j0}$ , and for  $\sigma'_3$  of 1 MPa, it will be 2.3 times of  $E_{j0}$ . This is likely to happen in field plate loading tests conducted underground on a limited surface area or when lateral in situ stress is not fully released.

The strength criterion for the jointed rocks when  $\sigma'_3$  is large compared to its tensile strength,  $\sigma_t$ , is given by

$$(\sigma'_1 - \sigma'_3)/\sigma'_3 = B_j(\sigma_{cj}/\sigma'_3)^{\alpha_j}, \quad (17)$$

where  $\sigma'_1$  and  $\sigma'_3$  are major and minor principal stresses, respectively,  $\sigma_{cj}$  is the uniaxial compressive strength of

jointed rock obtained from Eq. (9), and  $\alpha_j$  and  $B_j$  are strength parameters of the jointed rock. The values of  $\alpha_j$  and  $B_j$  are obtained from following equations.

$$\alpha_j/\alpha_i = (\sigma_{cj}/\sigma_{ci})^{0.5} \quad \text{and} \quad (18)$$

$$B_i/B_j = 0.13 \exp[2.04\alpha_j/\alpha_i], \quad (19)$$

where  $\alpha_i$  and  $B_i$  are the strength parameters obtained from triaxial tests on intact rock specimens from the failure criterion. When Eq. (17) has to be applied for the strength of rock mass along the periphery of excavation, i.e., when  $\sigma'_3 \triangleq 0$ , the tensile strength,  $\sigma_t$ , of rock mass has to be considered in the denominator along with  $\sigma_3$  as per the original expression for the strength of rock. One way to assess  $\sigma_t$  for rock mass would be to consider proportional reduction of  $\sigma_t$  from the intact rock value, similar to the proportional reduction in compressive strength of intact rock.

## 8 Analyses of Field Cases with $J_f$ Relations

Using the strength, modulus and failure strain relations for rock mass with  $J_f$  and the corresponding values of intact rock, a few cases were analyzed by Sitharam et al. (2001), Sridevi and Sitharam (2000), Sitharam and Madhavi Latha (2002) and Arunakumari and Latha (2007). The model has been applied to two large power station caverns, one in Japan and the other in the Himalayas and to a slope at Kiirunavaara mine in Sweden. Slope stability analysis of the right abutment (359 m high) at Kauri side of Chenab river between Katra and Laole, Jammu and Kashmir, India, was carried out using joint factor model by Sitharam et al. (2005) and Sitharam and Maji (2007). By constructing an artificial neural network (ANN) model, stress–strain response and variation of  $E_j/E_i$  with  $J_f$  were predicted by Garaga and Latha (2010) for jointed rocks, by specifying intact rock properties,  $\sigma_3$ ,  $J_f$  and axial strain as inputs. Out of number of cases presented by them, typical stress–strain curves predicted by equivalent continuum (ECM) and ANN models for block jointed gypsum plaster are presented in Fig. 4. Figure 5 shows the predictions as per ANN with joint factor model compared with the experimental results of Agra sandstone.

## 9 Standup Time with Modulus Ratio

By considering the major factors which are actively responsible to control the standup time, the following expression was developed by Ramamurthy (2007) for a uniform formation without any adverse geological structures.

**Fig. 4** Comparison of stress–strain curves predicted by ECM and ANN with experimental values for block jointed Gypsum Plaster (data from Brown and Trollope 1970)

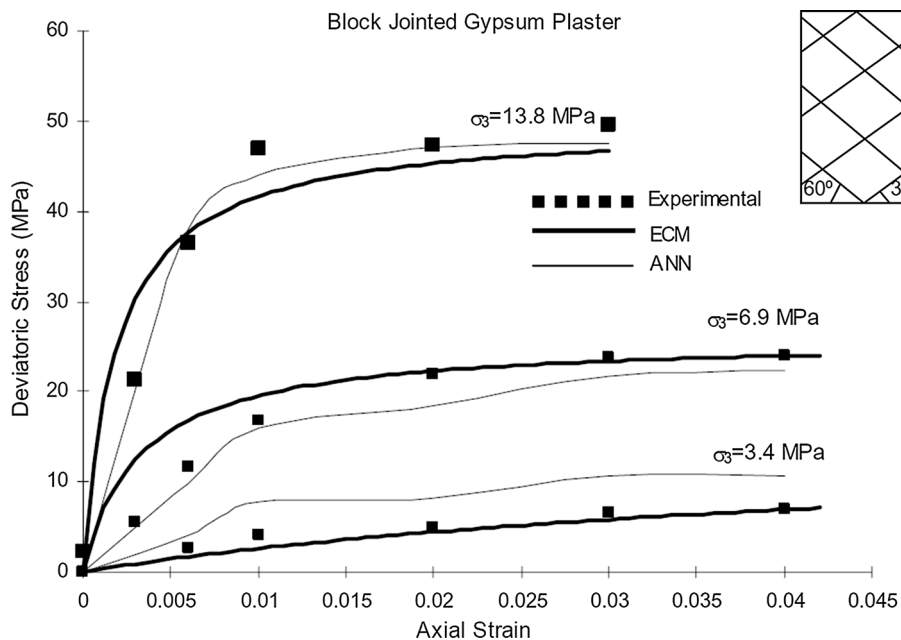
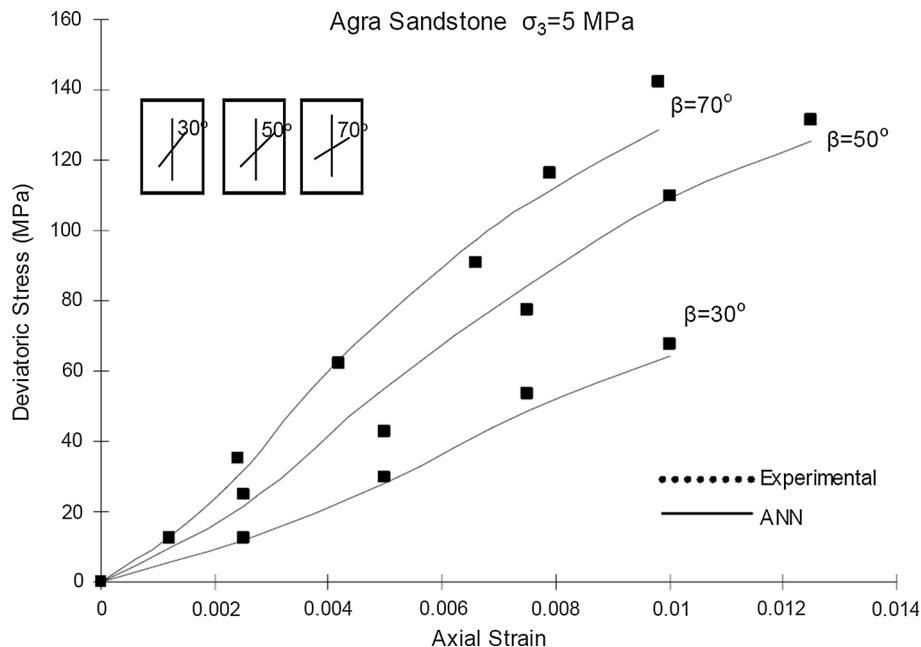


**Fig. 5** Effect of joint orientation on the stress strain response of Agra sandstone (data from Arora 1987)



$$t_f = \frac{k_s M_{rj}}{S_u (p_0 + u)} \tag{20}$$

where  $M_{rj}$  = modulus ratio of rock mass,  $S_u$  = effective span in meters,  $P_0$  = maximum in situ stress in  $t/m^2$ ,  $u$  = seepage pressure in  $t/m^2$ ,  $k_s$  = constant linked to  $M_{rj}$  (Table 12),  $t_f$  = standing time in years.

The value of  $k_s$  reflects the combined influence of blasting, shape of tunnel face, its orientation with respect to the joint system and also for converting  $t_f$ , the standup time, into years.

A number of cases have been examined for different diameters of tunnel, in situ stress, seepage pressure in very strong to very weak rock masses. The results are meaningful, comparable and acceptable and cover the range of values given under the limiting boundaries indicated by Bieniawski (1993). To obtain safe working values, one may apply a factor of safety of 2 or 3 either to the unsupported span or to the standup time, depending upon the openness of the joints, existence of joints parallel to the direction of excavation and the extent of loosening of immediate rock mass due to blasting operation. For values of  $t_f$ , estimated

**Table 12** Suggested values of constant,  $k_s$ , Ramamurthy (2007)

$M_{rj}$	500	200	100	50
$k_s$	100	5	1/5	1/100

from Eq. (20), less than an hour, an immediate collapse of rock mass from the crown may be expected.

### 10 Penetration Rate of TBM

Whether it is in  $Q_{TBM}$ , RMR or any other rock mass classification linked to penetration rate of tunnel boring machine (TBM),  $P_R$ , the modulus of rock has been ignored. For producing indentation by crushing under the tip of the cutter, compressive and tensile strengths of intact rock are important. The overall deformation or penetration produced will depend on the modulus and compressive strength of rock mass, more precisely to account for their combined influence  $M_{rj}$  has to be considered. Basically, under each cycle of boring by TBM, the various other major factors which control  $P_R$  are included in the following Eq. (21) given by Ramamurthy (2008). This equation is dimensionally correct and predicts  $P_R$  value per meter of advance of boring.

$$P_R = \frac{(T/A) \cdot (\sigma_{ci}/\sigma_{ti}) \cdot R \cdot N \cdot (DRI/100) \cdot s}{p_o \cdot M_{rj}}, \text{ m/h} \quad (21)$$

where  $T$  = net thrust, T;  $A$  = area of the cutter head,  $m^2$ ;  $\sigma_{ci}$  = compressive strength of intact rock, MPa;  $\sigma_{ti}$  = tensile strength of intact rock, MPa;  $R$  = number of rotations of cutterhead, per hour;  $N$  = number of cutters, per  $m^2$ ; DRI = drilling rate index based on compressive strength of intact rock,  $\sigma_{ci}/\sigma_{ti}$  as per NTH (1988);  $s$  = Unit length of drilling, i.e., 1.0 m;  $p_o$  = mean biaxial stress on the cutting face,  $T/m^2$  (or taken as density of rock mass times over burden height);  $M_{rj}$  = modulus ratio of rock mass.

In Eq. (21), the influence of seepage pressure is not considered, since most of the seepage pressure is dissipated at the cutting face due to the presence of fractures, joints,

etc. The seepage pressure acting through the intact rock will be negligible anyway on the cutting face. The rock parameters are to be obtained under saturated condition, if seepage exists.

The ratio  $(\sigma_{ci}/\sigma_{ti})$  takes care of inherent anisotropy in the intact rock and also its brittleness. When the gouge material thickness is less than 5 mm, the blocks formed in the rock mass may remain tight/interlocked and may not get dislodged during boring operation. But when the gouge material thickness is more than 5 mm, rock blocks may get dislodged and may damage the cutters. To take into consideration the thickness of gouge in the estimation of  $J_f$ , an equivalent number of joints are estimated by dividing the thickness of gouge (in mm) by 5 mm, which is the minimum thickness of gouge to be effective (Ramamurthy 2004).

Excellent data were collected by Sapigni et al. (2002) from NW Alps for metabasite in Maen tunnel and for micaschist and metadiorite in Pieve tunnel for various values of RMR which were estimated in front of the cutter head. These data were applied to verify Eq. (21). The RMR values have been converted to  $J_f$ , Joint factor, as per Eqs. (22) without ground water rating in RMR, as per Ramamurthy (2004)

$$J_f = 5(100 - RMR). \quad (22)$$

Minimum and maximum values of compressive strength, tensile strength and modulus of intact rocks, including the RMR of the rock masses for 16 types of rocks, were presented by Sapigni et al. (2002). This study also presented the details of the TBM adopted. Using this data, minimum, average and maximum values of  $M_{rj}$  were estimated. From  $J_f$  and  $M_{rj}$ , the minimum, average and maximum values of  $P_R$  were obtained. The values of  $P_R$  for minimum, average and maximum values of  $M_{rj}$  were calculated and presented (Ramamurthy 2008). A comparison of the calculated and field measured mean  $P_R$  values for 16 rock types with different rock mass quality, clearly suggested a good agreement. Only the  $P_R$  values for mica schist in Pieve tunnel calculated by Ramamurthy (2008) are given in Table 13.

**Table 13** Pieve tunnel, mica schist, rock mass density—2.6  $T/m^3$ ; average overburden—500 m; cutterhead rotation—678 rph (Ramamurthy 2008)

RMR	Joint factor $J_f$ per m	$P_R$ , m/h from Eq. (21)			Actual range $P_R$ , m/h
		Min. $M_{rj}$	Avg. $M_{rj}$	Max. $M_{rj}$	
83	85	1.7	1.7	1.5	1.2–2.2
75	125	2.0	1.9	1.8	1.6–2.5
68	160	2.4	2.2	2.0	2.0–2.8
57	215	2.7	2.7	2.4	2.1–3.3
50	250	3.0	3.1	2.8	2.3–3.4
35	325	3.9	4.0	3.5	2.5–3.5

The special advantage of adopting Eq. (21) for predicting  $P_R$  is that all the input data are factual and from test conducted on the rocks as per approved practice. It is dimensionally correct compared to other prevailing expressions. The  $P_R$  (m/h) may be calculated per meter of boring in a specified length having similar formation. Assessment of  $P_R$  per meter length of tunnel is specified because the  $J_f$  value is estimated per meter length. On the basis of this, one could estimate average  $P_R$  in each zone and then an overall estimation of the  $P_R$  or for the entire length of the tunnel can be carried out.

## 11 Conclusions

Modulus ratio concept defines the quality of intact rock and rock masses comprehensively by considering the compressive strength, modulus and failure strain in an unconfined state. A critical examination of the most commonly adopted rock mass classifications, namely, RMR, Q and GSI, has revealed that the values of compressive strength and modulus values suggested do not satisfy the modulus ratio concept. In some recent case studies presented, the modulus ratios of rock masses have been found to be much higher than those of the corresponding intact rocks. The joint factor concept developed based on actual tests suggests that the modulus ratio of rock mass has to be less than that of the corresponding intact rock. Application of this concept to predict the response of rocks in underground works and also for laboratory test specimens has been satisfactory. The modulus ratio and joint factor concepts have also been suggested to define soil–rock boundary in addition to compressive strength in unconfined state. The concept of modulus ratio was also applied to present a single classification applicable to intact rocks and rock masses, to predict standup time in underground excavations and also penetration rate of TBM.

## References

- Arora VK (1987) Strength and deformational behaviour of jointed rocks. Ph.D. thesis, Indian institute of Technology Delhi, India
- Arunakumari G, Latha GM (2007) Effect of joint parameters on stress–strain response of rocks. In: Proceedings of the 11th international congress ISRM, Lisbon, vol 1, pp 243–246
- Barla G (1993) Case study of rock mechanics in Masua mine, Italy. In: Hudson JA (ed) Comprehensive rock engineering, vol 5. Pergamon Press Ltd., Oxford, pp 291–334
- Barton N (2002) Some new Q-value correlations to assist in site characterisation and tunnel design. *Int J Rock Mech Min Sci Geomech Abstr* 39(2):185–216
- Barton N, Lien R, Lunde J (1974) Engineering classification of rock masses for the design of tunnel support. *J Rock Mech* 6(4):189–236
- Bieniawski ZT (1973) Engineering classification of jointed rock masses. *Transactions of the South African Institution of Civil Engineers* 5, vol 12, pp 335–344
- Bieniawski ZT (1976) Rock mass classification in rock engineering. In: Bieniawski ZT (ed) Proceedings symposium on exploration for rock engineering, vol 1. A.A. Balkema, Rotterdam, pp 97–106
- Bieniawski ZT (1993) Classification of rock masses for engineering: the RMR system and future trends. In: Hudson JA (ed) Comprehensive rock engineering, vol 3. Pergamon Press, Oxford, pp 553–573
- Bronshsteyn VI, Zhukov VN, Yufin SA, Zertsalov MG, Ustinov DV (2007) Rock mass behavior during a period of interrupted excavation and completion of caverns. In: Proceedings of the 11th International Congress ISRM, Lisbon, vol 2, pp 1015–1018
- Brown ET, Trollope DH (1970) Strength of model of jointed rock. *J ASCE* 96(SM2):685–704
- Carvalho JL, Kennard DT, Lorig L (2002) Numerical analysis of east wall of Toquepala mine, Southern Andes of Peru. In: Proceedings of the EUROCK, Lisbon, pp 615–625
- Clark IH (2006) Simulation of rock mass strength using ubiquitous joints. In: Hart R, Varona P (eds) Proceedings of the 4th international FLAC symposium on numerical modeling in geomechanics. Paper: 08-07, Minneapolis, USA
- Deere DU, Miller RP (1966) Engineering classification and index properties for intact rocks. Tech. Report no. AFNL-TR-65-116, Air Force Weapons Laboratory, New Mexico
- Garaga A, Latha GM (2010) Intelligent prediction of stress–strain response of intact and jointed rocks. *Comput Geotech* 37:629–637
- Gupta AS, Rao KS (2000) Weathering effects on the strength and deformational behaviour of crystalline rocks under uniaxial compression state. *Int J Eng Geol* 56:257–274
- Hobbs NB (1975) Factors affecting the prediction of settlement of structures on rock: with particular reference to chalk and Trias in settlement of structures. In: Proceedings of the conference on settlement of structures, Prentech. Press, pp 579–610
- Hoek E (1994) Strength of rock and rock masses. *ISRM News J* 2(2):4–16
- Hoek E, Brown ET (1997) Practical estimates of rock mass strength. *Int J Rock Mech Min Sci* 34(8):1165–1186
- Hoek E, Diederichs MS (2006) Empirical estimation of rock mass modulus. *Int J Rock Mech Min Sci* 43(2):203–215
- Hoek E, Moy D (1993) Design of large power house caverns in weak rocks. In: Hudson JA (ed) Comprehensive rock engineering, Pergamon Press Ltd., Oxford, vol 5, pp 85–110
- Hoek E, Carranza-Torres C, Corkum B (2002) Hoek-Brown failure criterion-2002 edition. In: Proceedings of the 5th North American rock mechanics symposium, Toronto, Canada, vol 1, pp 267–273
- Lim H, Kim CH (2003) Comparative study on the stability analysis methods for underground pumped power house caverns in Korea. In: Proceedings of the 10th international congress on ISRM, Johannesburg, vol 2, pp 783–786
- Lorig LJ (2007) Using numbers from Geology, Keynote Lecture. In: Proceedings of the 11th international congress on ISRM, Lisbon, vol 3, pp 1367–1377
- Moretto O, Pistone RES, DelRio JC (1993) A case history in Argentina—rock mechanics for underground works in pump storage development of Rio Grande No. 1. In: Hudson JA (ed) Comprehensive rock engineering, vol 5. Pergamon Press Ltd., Oxford, pp 159–192
- Natau O, Fliege O, Mutschler TH, Stech HJ (1995) True triaxial tests of prismatic large scale samples of jointed rock masses in laboratory. In: Proceedings of the 8th international congress rock mechanics, Tokyo, vol 1, pp 353–358

- NTH (Norwegian Institute of Technology) (1988) Hard rock tunnel boring, Project Report. Trondheim, Norway, pp 1–88
- Ramamurthy T (1993) Strength and modulus responses of anisotropic rocks. Chapter 13. In: Hudson JA (ed) *Comprehensive rock engineering*. Pergamon Press, Oxford, pp 313–329
- Ramamurthy T (2001) Shear strength responses of some geological materials in triaxial compression. *Int J Rock Mech Min Sci* 38:683–697
- Ramamurthy T (2004) A geo-engineering classification for rocks and rock masses. *Int J Rock Mech Min Sci* 41(1):89–101
- Ramamurthy T (2007) A realistic approach to estimate stand-up time. In: *Proceedings of the 11th congress on ISRM, Lisbon, vol 2*, pp 757–760
- Ramamurthy T (2008) Penetration rate of TBM. In: *Proceedings of the world tunnelling congress, Agra, India, vol 3*, pp 1552–1563
- Ramamurthy T, Arora VK (1994) Strength prediction for jointed rocks in confined and unconfined states. *Int J Rock Mech Min Sci* 13(1):9–22
- Read JRL (2008) Large open pit project, Keynote Lecture. In: *Proceedings of the International Symposium and 6 ARMS, New Delhi, India*, pp 119–131
- Richards L, Read SAL (2007) New Zealand Greywacke characteristics and influences on rock mass behaviour. In: *Proceedings of the 11th ISRM congress Lisbon, Portugal, vol 1*, pp 359–364
- Rocha M (1964) Mechanical behaviour of rock foundations in concrete dams. In: *Transactions of the 8th congress on large dams, Edinburgh, paper R-44, Q.28*, pp 785–832
- Sapigni M, Berti M, Bethaz E, Busillo A, Cardone G (2002) TBM performance estimation using rock mass classifications. *Int J Rock Mech Min Sci* 39:771–788
- Sari M, Karpuz C, Ayday C (2010) Estimating rock mass properties using Monte Carlo simulation: ankara andesites. *Comput Geosci* 36:959–969
- Serafim JL, Pereira JP (1983) Consideration of the geomechanics classification of Bieniawski. In: *Proceedings of the International Symposium on Engineering, Geology and Underground Construction, Lisbon, Portugal*, pp 33–44
- Ermekov TM, Abuov MG, Shashkin, VN, Freidin AM, Uskov VA (1985) Providing of stability of horizontal mine working in soft rock. In: *Proceedings of the 8th international congress on ISRM, Japan, vol 2*, pp 671–674
- Singh M, Rao KS, Ramamurthy T (2002) Strength and deformational behaviour of a jointed mass. *J Rock Mech Rock Eng* 35(1):45–64
- Sitharam TG, Latha GM (2002) Simulation of excavation in jointed rock masses using practical equivalent continuum model. *Int J Rock Mech Min Sci* 39:517–525
- Sitharam TG, Maji VB (2007) Slope stability analysis of a large slope in rock mass: a case study. In: *Proceedings of the 11th international congress on ISRM, Lisbon, Portugal, vol 2*, pp 1185–1188
- Sitharam TG, Sridevi J, Shimizu N (2001) Practical equivalent continuum characterization of jointed rock masses. *Int J Rock Mech Min Sci* 38:437–448
- Sitharam TG, Maji VB, Varma AK (2005) Equivalent continuum analyses of jointed rock mass. In: *40th US Rock Mechanics Symposium, Alaska, USA, Paper: 05-776*
- Sridevi J, Sitharam TG (2000) Analysis of strength and moduli of jointed rocks. *Geotech Geol Eng* 18:3–21
- Stabel B, Samani FB (2003) Masjed-e-soleiman hydroelectric power project, rock engineering investigations, analysis, design and construction. In: *Proceedings of the 10th international congress on ISRM, Johannesburg, vol 2*, pp 1147–1154
- Tabanrad R (2003) Monitoring and stability analysis of intake tunnels, Karun III hydroelectric power project. In: *Proceedings of the 10th international congress on ISRM, Johannesburg, vol 2*, pp 1189–1193
- Walsh JB, Brace WF (1966) Elasticity of rock: a review of some recent theoretical studies. *Rock Mech Eng Geol* 4(4):283–297
- Yu C, Liu SC (1993) Power caverns of Mingtan pumped storage project, Taiwan. In: Hudson JA (ed) *Comprehensive rock engineering*, vol 5. Pergamon Press Ltd., Oxford, pp 111–131
- Zhou Y, Zhao J, Cai JG, Zhang XH (2003) Behaviour of large—span rock tunnels and caverns under favourable horizontal stress conditions. In: *Proceedings of the 10th international congress on ISRM, Johannesburg, vol 2*, pp 1381–1386